UDC 551.509.313:551.511.32

An Efficient, One-Level, Primitive-Equation Spectral Model

WILLIAM BOURKE—*Commonwealth Meteorology Research Centre, Melbourne, Victoria, Australia*

ABSTRACT—A one-level, global, spectral model using the primitive equations is formulated in terms of a concise form of the prognostic equations for vorticity and divergence. The model integration incorporates a grid transform technique to evaluate nonlinear terms; the computational efficiency of the model is found to be far superior to that of an equivalent model based on the traditional interaction coefficients. The transform model, in integrations of 116 days, satisfies principles of conservation of energy, angular momentum, and square potential vorticity to a high degree.

1. INTRODUCTION

Numerical schemes for mathematical simulation of atmospheric flow commonly employ one of two methods. The more usual approach represents the dynamic meteorological variables in space and time on a finite-difference grid. An alternative method less commonly adopted represents the variance of these fields, in part, by truncated spectral expansions. In particular, a spectral representation for the horizontal variation of the dynamic fields over the globe offers a number of significant advantages. Foremost among these advantages is the elimination of aliasing in the evaluation of horizontal advection terms; in addition, the problems arising in global grids at the poles and in the alternative of mapping of the sphere do not occur. These and other advantages are well known and have been discussed by Platzman (1960), Kubota et al. (1961), Baer and Platzman (1961), Ellsaesser (1966), Robert (1966), Eliasen et al. (1970), and Orszag (1970). Until recently, these advantages have been largely overwhelmed by a serious problem with respect to the computational efficiency of the spectral approach in comparison to that of the grid method. Recently, Orszag (1970) has suggested a transform procedure whereby the computational efficiency of a spectral model can be much improved; while Eliasen et al. (1970) have demonstrated numerically, using a transform approach, that the efficiency of integration of the primitive meteorological equations in spectral form can be considerably enhanced.

The present study suggests a simple and concise form of the one-level primitive equations that can be readily integrated via a transform procedure when one specifies the horizontal variance of the dynamic fields by truncated expansions of orthogonal spherical harmonics. The spectral representation of these equations is presented together with results of numerical model integrations; a comparative study of this transform model and a model based on the more traditional spectral method demonstrates that a considerable improvement in computational efficiency arises from the transform technique.

The essence of the transform procedures proposed by Orszag (1970) and by Eliasen et al. (1970) is to evaluate the nonlinear terms of the equations as simple products following a transform from the spectral to gridpoint domain; a subsequent inverse transform yields the spectral form of the requisite nonlinear term. The procedure may be more generally described as combining nonlocal (spectral) differentiations with local (gridpoint) multiplications for evaluation of the nonlinear terms.

2. EQUATIONS OF MOTION

The equations of motion employed to simulate atmospheric flow are most appropriately applied to the atmosphere considered in depth. However, many of the mathematical properties of the equations are embodied in a simpler set of equations that describe motion of a free surface of a homogenous and incompressible fluid. It is this simpler set of equations, referred to variously as the free-surface equations or the one-level primitive equations, that is considered here as a means of illustrating a procedure of more general application.

The equations describing the motion of a free surface may be written as

$$\frac{d\mathbf{V}}{dt}=-f\mathbf{k}\times\mathbf{V}-\nabla\Phi \tag{1}$$

and

$$\frac{d\Phi}{dt}=-\Phi\nabla\cdot\mathbf{V} \tag{2}$$

where $\mathbf{V}$ is the horizontal wind vector with eastward and northward components of u and v, respectively, Φ is the geopotential height of the free surface, f is the Coriolis parameter, $\mathbf{k}$ is the vertical unit vector, ∇ is the horizontal gradient operator, and d/dt is the total time derivative.

The specification of such equations in the spectral domain has been discussed by Robert (1966) who noted that the components u and v of the vector wind constitute pseudoscalar fields on the globe and as such are not well suited to representation in terms of scalar spectral

expansions. Robert suggested that the variables

$$U=u\cos\phi$$

and

$$V=v\cos\phi,$$

where ϕ denotes latitude, would be more appropriate in the global spectral formulation. Accordingly, he performed a long-term integration of a multilevel primitive-equation model with U and V as the horizontal wind prognostics.

The horizontal wind field may, however, be equally well specified in terms of horizontal divergence and the vertical component of relative vorticity; these two quantities are scalars and are well suited as dynamic variables in a spectral model. On application of the curl ($\mathbf{k}\cdot\nabla\times$) and divergence operators ($\nabla\cdot$) to eq (1), expanded to the form

$$\frac{\partial\mathbf{V}}{\partial t}=-(\xi+f)\mathbf{k}\times\mathbf{V}-\nabla\left(\Phi+\frac{\mathbf{V}\cdot\mathbf{V}}{2}\right), \tag{3}$$

the prognostic equations for horizontal vorticity and divergence are found to be

$$\frac{\partial\xi}{\partial t}=-\nabla\cdot(\xi+f)\mathbf{V} \tag{4}$$

and

$$\frac{\partial D}{\partial t}=\mathbf{k}\cdot\nabla\times(\xi+f)\mathbf{V}-\nabla^2\left(\Phi'+\frac{\mathbf{V}\cdot\mathbf{V}}{2}\right). \tag{5}$$

The continuity equation [eq (2)] may be re-expressed in a form, similar to eq (4) and (5), as follows:

$$\frac{\partial\Phi'}{\partial t}=-\nabla\cdot\Phi'\mathbf{V}-\overline{\Phi}D. \tag{6}$$

Here, ξ is $\mathbf{k}\cdot\nabla\times\mathbf{V}$, the vertical component of relative vorticity, D is $\nabla\cdot\mathbf{V}$, the horizontal divergence, and the substitution of $\Phi=\overline{\Phi}+\Phi'$ denotes a time-independent global mean geopotential, $\overline{\Phi}$, and the time-dependent perturbation field, Φ'; this substitution facilitates subsequent semi-implicit time integration.

It is convenient now to invoke the theorem of Helmholtz and represent the wind vector $\mathbf{V}$ in terms of a stream function, ψ, and a velocity potential, χ, as

$$\mathbf{V}=\mathbf{k}\times\nabla\psi+\nabla\chi. \tag{7}$$

From eq (7), the quantities ξ and D are seen to be expressible as

$$\xi=\mathbf{k}\cdot\nabla\times\mathbf{V}=\nabla^2\psi \tag{8}$$

and

$$D=\nabla\cdot\mathbf{V}=\nabla^2\chi. \tag{9}$$

Expanding, in part, the vorticity, divergence, and continuity equations, as given by eq (4)–(6), into spherical, polar coordinates, substituting $U=u\cos\phi$ and $V=v\cos\phi$, and incorporating eq (8) and (9) yields

$$\frac{\partial}{\partial t}(\nabla^2\psi)=-\frac{1}{a\cos^2\phi}\left[\frac{\partial}{\partial\lambda}(U\nabla^2\psi)+\cos\phi\,\frac{\partial}{\partial\phi}(V\nabla^2\psi)\right]-2\Omega\left(\sin\phi\nabla^2\chi+\frac{V}{a}\right), \tag{10}$$

$$\frac{\partial}{\partial t}(\nabla^2\chi)=+\frac{1}{a\cos^2\phi}\left[\frac{\partial}{\partial\lambda}(V\nabla^2\psi)-\cos\phi\,\frac{\partial}{\partial\phi}(U\nabla^2\psi)\right]+2\Omega\left(\sin\phi\nabla^2\psi-\frac{U}{a}\right)-\nabla^2\left(\frac{U^2+V^2}{2\cos^2\phi}+\Phi'\right), \tag{11}$$

and

$$\frac{\partial\Phi'}{\partial t}=-\frac{1}{a\cos^2\phi}\left[\frac{\partial}{\partial\lambda}(U\Phi')+\cos\phi\,\frac{\partial}{\partial\phi}(V\Phi')\right]-\overline{\Phi}D \tag{12}$$

where λ, ϕ, and t denote the independent variables longitude, latitude, and time, respectively; a denotes the radius of the earth; and Ω is the rotation rate of the earth.

The quantities U and V appearing in eq (10)–(12) are not prognostic variables but may be derived from the simple linear relationship given by eq (7). Expanding eq (7) yields

$$U=-\frac{\cos\phi}{a}\frac{\partial\psi}{\partial\phi}+\frac{1}{a}\frac{\partial\chi}{\partial\lambda} \tag{13}$$

and

$$V=\frac{1}{a}\frac{\partial\psi}{\partial\lambda}+\frac{\cos\phi}{a}\frac{\partial\chi}{\partial\phi}. \tag{14}$$

The prognostic equations [eq (10)–(12)] together with the diagnostic expressions [eq (13) and (14)] constitute the form appropriate for the present study.

An advantage of the equations expressed as above is that they are concise. The actual number of fields involved in nonlinear products is less than is required in the form that employs U and V as the wind prognostics; it should be noted that this comparative simplicity is gained at the expense of some complexity in treating curl and divergence operators subsequent to formation of nonlinear products. The truncation procedure for these concise equations in spectral form is straightforward since the prognostic variables are scalars; in addition, the implementing of a semi-implicit time scheme is facilitated by the explicit prognostic for divergence.

3. THE EQUATIONS OF MOTION IN SPECTRAL FORM

The spectral approach has been commonly invoked to integrate the barotropic or nondivergent vorticity equation, there being one dynamic variable, namely, the stream function. Silberman (1954) represented the global variance of the stream function in terms of orthogonal spherical harmonics and demonstrated a procedure for numerical integration of the resulting prognostic spectral equations. Subsequently, Platzman (1960), Kubota et al. (1961), Baer and Platzman (1961), and Ellsaesser (1966) have all employed the approach of Silberman in integrations of the vorticity equation. The transformation of the vorticity equation into the spectral domain, as used by these authors, yields prognostics for spectral amplitude coefficients in terms of quadruple summations involving interaction coefficients. The rapid increase in the number of interaction coefficients as a function of increasing spectral resolution has been, in part, responsible for the inefficiency long associated with the spectral method.

Robert has suggested use of low-order spectral functions based on nonorthogonal elements of the spherical

harmonics; this method has been successfully applied in a multilevel primitive-equation model (Robert 1966) and in a nondivergent vorticity model (Robert 1968). This approach eliminates the troublesome complexity of interaction coefficients at the small expense of an orthogonalization procedure at each time step of numerical integration.

Eliasen et al. (1970) have demonstrated that spectral model integration of the primitive equations may be greatly facilitated by a spectral grid transform technique. A similar procedure has also been suggested by Orszag (1970) and discussed with reference to a nondivergent vorticity model. The essential, nontrivial aspect of a spectral model integration arises in evaluation of the nonlinear products, and it is the ready simplification of these spectral multiplications that is possible via the transform method. The transform technique requires:

1. A transform of appropriate spectral fields to a spatial grid
2. Multiplication of grid values point by point.
3. An inverse transform on the product formed at gridpoints to revert to the spectral domain.

Equations (10)–(12) have been derived so as to facilitate incorporation of a transform method in a global spectral model. A spectral representation of eq (10)–(12) is readily given in terms of orthogonal spherical harmonics as used by Silberman (1954). These harmonics are eigenfunctions of the Laplacian operator, ∇^2, and are thus appropriate for use in the equations as presented. Truncated expansions for approximating the stream function, velocity potential, geopotential height, and two derived wind fields are required. These expansions, in terms of time-dependent amplitudes, are

$$\psi=a^2\sum_{m=-J}^{+J}\sum_{l=|m|}^{|m|+J}\psi_l^m Y_l^m,$$

$$\chi=a^2\sum_{m=-J}^{+J}\sum_{l=|m|}^{|m|+J}\chi_l^m Y_l^m, \quad (15)$$

$$\Phi=a^2\sum_{m=-J}^{+J}\sum_{l=|m|}^{|m|+J}\Phi_l^m Y_l^m, \quad (16)$$

$$U=a\sum_{m=-J}^{+J}\sum_{l=|m|}^{|m|+J+1}U_l^m Y_l^m,$$

$$V=a\sum_{m=-J}^{+J}\sum_{l=|m|}^{|m|+J+1}V_l^m Y_l^m \quad (17)$$

where

1. The terms ψ_l^m and so forth denote time-dependent generally complex expansion coefficients; the reality of the fields requires $(\psi_l^m)^*=(-)^m\psi_l^{-m}$ and so forth.

2. $Y_l^m=P_l^m(\sin\phi)e^{im\lambda}$; $P_l^m(\sin\phi)$ is an associated Legendre polynomial of the first kind (normalized to unity; that is,

$$\int_{-\pi/2}^{+\pi/2}P_l^m(\sin\phi)\,P_l^m(\sin\phi)\cos\phi d\phi=1$$

of degree l and order m.

3. The truncation parameter, J, denotes rhomboidal wave number truncation (Ellsaesser 1966), m denotes a planetary wave number, and $(l-m)$ denotes a meridional wave number.

In expressing the U- and V-fields spectrally, it is essential that these derived wind fields be identical to those implied by the truncated expansions for ψ and χ. Substitution of the expansions of eq (15) and (17) into eq (13) and (14) yields, on application of a standard recurrence relation and the orthogonality property of the harmonics, the relationships

$$U_l^m=(l-1)\epsilon_l^m\psi_{l-1}^m-(l+2)\epsilon_{l+1}^m\psi_{l+1}^m+im\chi_l^m \quad (18)$$

$$V_l^m=-(l-1)\epsilon_l^m\chi_{l-1}^m+(l+2)\epsilon_{l+1}^m\chi_{l+1}^m+im\psi_l^m \quad (19)$$

where

$$\epsilon_l^m=\sqrt{(l^2-m^2)/(4l^2-1)}.$$

It becomes apparent from eq (18) and (19) that expansions for U and V must, as implied in eq (17), extend to one degree above that defined in eq (15) for ψ and χ;[1] for example, nonzero values of $U_{|m|+J+1}^m$ are implied by variance in $\psi_{|m|+J}^m$.

In eq (10)–(12), the nonlinear products occurring are $U\nabla^2\psi$, $V\nabla^2\psi$, $U\Phi'$, $V\Phi'$, and $(U^2+V^2)/2$. The spectral evaluation of these nonlinear terms may be accomplished by

1. A transform of spectral fields of U, V, $\nabla^2\psi$, and Φ' to a two-dimensional (latitude-longitude) grid on the globe.[2]
2. Evaluation of the above terms at each gridpoint.
3. An inverse transform of these terms.

The requisite inverse transforms involve the curl and divergence operators, and, as an example of the procedure, the vorticity equation is considered in detail below. Having obtained the gridpoint values of $U\nabla^2\psi$ and $V\nabla^2\psi$, it is appropriate to represent these gridpoint values in terms of truncated Fourier series at each latitudinal circle as follows:

$$U\nabla^2\psi=a\sum_{m=-J}^{+J}A_m e^{im\lambda}$$

and (20)

$$V\nabla^2\psi=a\sum_{m=-J}^{+J}B_m e^{im\lambda}.$$

The Fourier amplitudes A_m and B_m are obtained by inverse transformation. After substituting eq (20) together with (15) into the vorticity equation and again using the orthogonality property of the spherical harmonics, the spectral prognostic is seen to be, in part, a function of the

[1] There is an implication in eq (18) and (19) that is pertinent to spectral models employing U and V as prognostic variables. As Robert (1966) showed and as discussed in detail by Eliasen et al. (1970), the truncation of tendencies for components U_l^m and V_l^m is found to be well behaved if made equivalent to a truncation of tendencies for the ψ- and χ-fields. A satisfactory truncation for the true scalar fields such as ψ and χ is achieved simply by evaluating tendencies only for those components initially considered in the expansions; such an approach in a nondivergent vorticity model conserves, apart from errors due to time truncation and roundoff, quadratic invariants of energy and square vorticity. To achieve a satisfactory truncation with U_l^m and V_l^m as prognostic variables one must make corrections to the highest degree components for each order (Eliasen et al. 1970).

[2] The approach of Eliasen et al. (1970), employing U and V as the wind prognostics, employs a transform of requisite fields to a latitudinal grid only; the multiplication of various Fourier series is then performed spectrally. This one-dimensional transform achieves the primary and important aim of elimination of interaction coefficients; a full two-dimensional transform is adopted in the present study and has also been employed by the above authors (Machenhauer 1971).

integral

$$\int_{-\pi/2}^{+\pi/2} \frac{1}{\cos^2\phi}\left(imA_m + \cos\phi \frac{\partial B_m}{\partial \phi}\right) P_l^m(\sin\phi)\cos\phi d\phi.$$

In the course of their particular truncation procedure, Eliasen et al. (1970) show that such an integral, upon integrating the second term by parts, may be exactly evaluated by applying Gaussian quadrature at a sufficient number of gridpoints. The spectral form of the vorticity equation, therefore, may be conveniently written as

$$-l(l+1)\frac{\partial \psi_l^m}{\partial t} = -\int_{-\pi/2}^{+\pi/2} \frac{1}{\cos^2\phi}\left[imA_m P_l^m(\sin\phi) - B_m \cos\phi \frac{\partial P_l^m(\sin\phi)}{\partial \phi}\right]\cos\phi d\phi + 2\Omega[l(l-1)\epsilon_l^m \chi_{l-1}^m + (l+1)(l+2)\epsilon_{l+1}^m \chi_{l+1}^m - V_l^m]. \quad (21)$$

The spectral truncation of the evaluated tendencies is straightforward, as the variables are true scalars and tendencies are only required for those components within the spectral range defined by the truncation parameter, J.

A similar type of integral to that in eq (21) arises in considering the divergence and continuity equations. With additional representations analogous to those of eq (20), namely,

$$U\Phi' = a^3 \sum_{m=-J}^{+J} C_m e^{im\lambda},$$

$$V\Phi' = a^3 \sum_{m=-J}^{+J} D_m e^{im\lambda},$$

and

$$\frac{U^2+V^2}{2} = a^2 \sum_{m=-J}^{+J} E_m e^{im\lambda}, \quad (22)$$

the tendencies for the velocity potential and geopotential spectral amplitudes are found to be

$$-l(l+1)\frac{\partial \chi_l^m}{\partial t} = \int_{-\pi/2}^{+\pi/2} \frac{1}{\cos^2\phi}\left[imB_m P_l^m(\sin\phi) + A_m \cos\phi \frac{\partial P_l^m(\sin\phi)}{\partial \phi}\right]\cos\phi d\phi - 2\Omega[l(l-1)\epsilon_l^m \psi_{l-1}^m + (l+1)(l+2)\epsilon_{l+1}^m \psi_{l+1}^m + U_l^m] + l(l+1)(E_l^m + \Phi_l^m) \quad (23)$$

and

$$\frac{\partial \Phi_l^m}{\partial t} = -\int_{-\pi/2}^{+\pi/2} \frac{1}{\cos^2\phi}\left[imC_m P_l^m(\sin\phi) - D_m \cos\phi \frac{\partial P_l^m(\sin\phi)}{\partial \phi}\right]\cos\phi d\phi + \bar{\Phi} l(l+1)\chi_l^m \quad (24)$$

where

$$E_l^m = \int_{-\pi/2}^{+\pi/2} \frac{E_m}{\cos^2\phi} P_l^m(\sin\phi)\cos\phi d\phi. \quad (25)$$

Thus, eq (21), (23), (24), and (25) constitute the requisite spectral form of the free-surface equations.

For the transform procedure to be equivalent to that in which spectral multiplications are evaluated nonlocally, the gridpoint multiplications must be free of aliasing. Orszag (1970) pointed out that $4J$ equispaced points around each latitude circle would allow alias-free evaluation of Fourier transforms such as occur in eq (20) and (22). Orszag (1971) has more recently discussed an improved transform procedure, as has Machenhauer (1971), and it is apparent from these authors that $(3J+1)$ equispaced longitudinal gridpoints are sufficient to ensure alias-free evaluation of the Fourier transforms considered here.

Eliasen et al. (1970) have discussed in some detail the requirement of resolution in the meridional direction for performing exact integrations via Gaussian quadrature. It is sufficient to note here that the integrands occurring in eq (21), (23), (24), and (25) are polynomials of at most degree $5J$; since Gaussian quadrature applied over K angles is exact for any polynomial of degree less than or equal to $(2K-1)$, a grid of $(5J+1)/2$ Gaussian angles of latitude is sufficient for exact integration.

4. NUMERICAL INTEGRATIONS

A computer code has been developed to numerically integrate the spectral tendency equations [eq (21), (23), (24), and (25)]; the spectral truncation chosen is rhomboidal as indicated in eq (15). The code has employed the fast-Fourier transform subroutine of Brenner (1969) and the procedures of Belusov (1962) for generating the requisite associated Legendre polynomials. The advantages inherent in usage of a fast-Fourier algorithm have been discussed by Orszag (1970). The time integration is implemented by the standard leapfrog scheme with, however, Φ_l^m of eq (23) and χ_l^m of eq (24) considered implicitly; this semi-implicit method developed by Robert (1969) permits, at the expense of inaccuracies in the phase speed of gravity waves, a time step of approximately six times the value acceptable in a fully explicit approach. A modified Euler-backward time step (Kurihara 1965) provides a smooth start and also removes the computational mode when periodically applied.

A first evaluation of the model, coded as above, employed the initialization procedure suggested by Phillips (1959); the stream function was specified in terms of a particular analytic solution of the nondivergent vorticity equation with the geopotential corresponding to the solution of the reverse nonlinear balance equation. In a divergent model, as considered here, it is expected that the solution of the equations will differ, at least initially, only slightly from the analytic nondivergent case. In particular, as also found by Grimmer and Shaw (1967), the numerically calculated phase speed is found to be a little less than that of the analytic solution. With similar initialization and constants as Grimmer and Shaw (1967), a numerical integration ($J=10$) over a period of 96 hr yielded a phase speed of 9.2°/day. The analytic solution yields a phase speed of 9.6°/day.

A more appropriate test of the numerical integrations is provided on initializing the dynamic fields with real data and thereby allowing the nonlinear terms realistic significance. Correspondingly, all subsequently described numerical integrations have been performed with an initial global stream function, as given in the spherical harmonic

TABLE 1.—*Transform model timing*

Wave number truncation, J (rhomboidal)	Transform grid		Computation time/time step (s)
	Number of Gaussian latitudes	Number of points per latitude circle	
7	20	24	2. 3
12	32	48	7. 8
15	40	48	12. 2
24	64	96	39
30	80	96	67

TABLE 2.—*Interaction coefficient timing*

Wave number truncation, J (rhomboidal)	Number of interaction coefficients*	Computation time/time step (s)
5	3, 657	1. 1
7	16, 250	4. 2
10	83, 169	18. 6
13	283, 577	59
15	558, 276	114

*Comprising interaction coefficients arising from scalar triple products and from ordi nary products

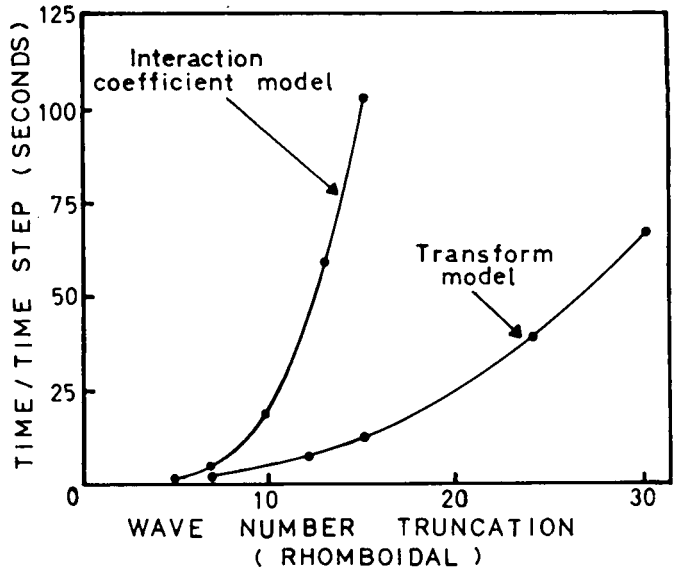

FIGURE 1.—Computation time per time step (s) as a function of spectral resolution. Integrations of a global spectral model employing a transform method and employing the interaction coefficient method are compared.

analysis of Merilees (1968*a*) for the 500-mb IGY data. With the stream function so specified, a geopotential field can be derived by imposing the balance condition $\partial D/\partial t=0$; as the semi-implicit time scheme is being used, a first time step correction yields slightly better balance of the fields.

The overall efficiency of the transform model was of prime interest, and the computation time per time step was measured as a function of the wave number truncation parameter, J. For comparative purposes, the same information was measured for integrations of an equivalent free-surface model formulated in terms of the fully differentiated equations and requiring interaction coefficients. This interaction coefficient model has been coded by the author, as with the transform model, with the same limited degree of coding optimization; the formulation was based on that given by Merilees (1968*b*) for the primitive meteorological equations.[3] Table 1 displays timing information for the transform model and the corresponding resolution of the transform grids. Table 2 displays timing information for the interaction coefficient model and the number of requisite interaction coefficients. These timing results are all graphed in figure 1. A considerable gain in efficiency is apparent from use of the transform approach; the interaction coefficient model displays the well-known increase in the number of requisite interaction coefficients and corresponding catastrophic loss of efficiency as a function of increasing spectral resolution. The timing for the interaction coefficient model was derived from calculations in which one constant interaction coefficient was continually accessed; the model has been correctly integrated for $J\leq 10$, but the number of coefficients becomes prohibitive in a real calculation for $J>10$.

The limitation of the efficiency of the transform model with increasing spectral resolution is related to the time required to perform transforms of the associated Legendre expansions. The ratio of computation time required for Fourier transforms to that required for Legendre transforms decreases from 1.0 at truncation of $J=15$ to 0.5 at truncation of $J=30$; the lack of a fast algorithm to perform the Legendre transforms is becoming apparent at $J=30$.

Both models considered here employed level-H Fortran and were run on an IBM 360/65 [4] computer having available 200,000 bytes of core; the codes employ single precision arithmetic, although the requisite associated Legendre polynomials are generated in double precision for the transform model at each time step.

The free-surface equations denoted by eq (1) and (2) embody, among others, principles of conservation of energy, angular momentum, and square potential vorticity. The extent to which the numerical model integrations satisfy such principles has long been a criterion in evaluating the stability, not to be confused with accuracy, of various numerical schemes. These conservation principles may be expressed as constraints on the integrals over the mass field of the fluid for the quantities, given per unit mass, of

$$\text{energy} = \frac{U^2+V^2}{2\cos^2\phi}+\Phi',$$

$$\text{angular momentum} = a\,(U+\Omega\, a\cos^2\phi),$$

and

$$\text{square potential vorticity} = g^2\left(\frac{\nabla^2\psi+f}{\Phi}\right)^2.$$

[3] The evaluation of nonlinear terms in the interaction coefficient model incorporated the procedure of Baer and Platzman (1961) but with the minor omission of the economy available in explicit storage of the four-component multiplications implied by multiplication of two complex amplitudes. The prognostic equations were manipulated to contain interaction coefficients corresponding to scalar triple products and ordinary products; use of appropriate selection rules eliminated the majority of null interactions.

[4] Mention of a commercial product does not constitute an endorsement.

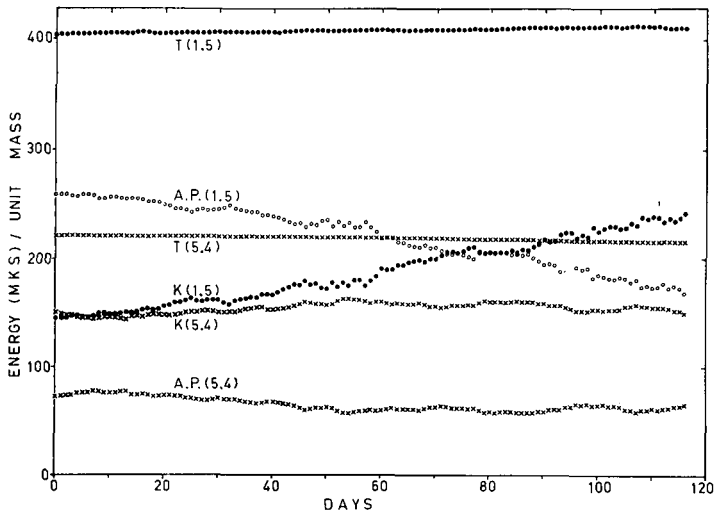

FIGURE 2.—Energetics of two long-term integrations of the transform model. The integrations differ only in definition of mean free-surface height. K, A.P., and T denote global integrals of kinetic energy, available potential energy, and total available energy for the two values of mean free-surface height of 1.5 and 5.4 km.

The conservation of mass in the present spectral model is implicit, as the tendency of the global mean geopotential field is identically zero.

As a more extensive test of the transform model, two, long-term numerical integrations have been performed. These integrations have been performed with a spectral truncation of wave number $J=15$; the global 500-mb spectral analysis of Merilees (1968*a*) provided the stream function at resolution of $J=15$. The geopotential field obtained by initializing the model is a little removed from reality—the initial stream function was obtained through a spectral form of the linear balance equation and, for the present purposes, this stream function was used in the reverse nonlinear balance equation to generate a balanced geopotential. The two calculations were both initialized with the stream function from the global spectral analysis for Sept. 6, 1957; these two calculations, subsequently denoted by A and B, differed only in that mean free-surface heights of 1.5 and 5.4 km, respectively, were employed. In both A and B, the transform grid was defined by 64 points around each of 40 Gaussian latitudes; a semi-implicit time scheme permitted 1-hr time steps, and a modified Euler-backward time step (Kurihara 1965) was applied once at 8-day intervals in A and at 4-day intervals in B to remove the computational mode.

During the 116-day period, the principles of conservation of available energy, angular momentum, and square potential vorticity were well satisfied. Figure 2 displays the energetics of both integrations, at 1-day intervals, for the 116-day period. The global integrals of available energy, angular momentum, and square potential vorticity varied in the 116-day period by $+2$, -0.01, and -4 percent, respectively, in A, and by -3, $+0.4$, and -0.7 percent, respectively, in B. In evaluation of the kinetic energy integral, E_7^m is truncated prior to integration over the mass field; evaluation of square potential vorticity is obtained from an inverse transform of grid-point values to avoid an explicit spectral division. As a measure of the extent to which divergence had developed in the model, the ratio of the root-mean-square (rms) amplitude of divergence to the rms amplitude of vorticity was calculated; in A this ratio grew to 5.5 percent and in B, to 3 percent. The differing behavior of the energy conversions in these two calculations is consistent with enhancement of divergence arising in A; the extent to which energy conversions may be influenced by semi-implicit time integration remains to be examined.

As already discussed, the numerical integration of a nondivergent barotropic spectral model can exactly conserve, apart from small errors arising from roundoff and time truncation, the quadratic invariants such as energy and square vorticity. Whether or not exactness of related constraints applies in the divergent barotropic (i.e., the free-surface) spectral model requires further analysis as the constraints reduce to integrals of greater complexity than quadratic and for which the presently adopted truncation scheme may strictly be less appropriate. However, it has been found in the present study and by Eliasen et al. (1970) that such integral constraints in practice are satisfied to a high degree in a divergent barotropic spectral model.

5. CONCLUSIONS

The recently suggested principle of evaluating nonlocal spectral products in local gridpoint space (Orszag 1970, Eliasen et al. 1970) considerably enhances the efficiency of numerical integration of the free-surface equations via the spectral method. In comparison to the more traditional spectral method, it has been shown that an order-of-magnitude improvement in efficiency is obtained by the transform method even at relatively low spectral truncation of wave number 15. In addition, the capability of the spectral method has been considerably enlarged by this development, as much higher spectral resolution is now feasible.

The present study has presented a concise form of the set of free-surface (primitive) equations that may be readily transformed and integrated in the spectral domain. long-term integration of these equations was found to be stable, satisfying to a high degree several of the conservation principles embodied in the differential equations. Both a semi-implicit time scheme and the spectral truncation of the tendency fields are readily implemented with the equations in the form suggested. The extension of the present formulation to a multilevel primitive equation model of atmospheric flow does not appear to present major difficulties, and a five-level σ-coordinate model has been coded and is currently being tested. The use of a three-dimensional grid at an intermediate point in each time step of the integration should facilitate the inclusion of effects that are not so readily treated in the spectral domain such as moisture and radiation.

ACKNOWLEDGMENTS

The author gratefully acknowledges use of the computing facilities of the Canadian Meteorological Service; the coding of the transform model and initial numerical integrations were carried out by the author while visiting the Dynamic Prediction Unit in Montreal. In addition, the author would like to thank André Robert for many informative discussions relating to spectral models. A coding of Belusov's associated Legendre generation by J. H. Bradley and the IGY analysis by P. Merilees were available to the author from the Department of Meteorology, McGill University, Montreal.

REFERENCES

Baer, Ferdinand, and Platzman, George W., "A Procedure for Numerical Integration of the Spectral Vorticity Equation," *Journal of Meteorology*, Vol. 18, No. 3, June **1961**, pp. 393–401.

Belusov, S. L., "Tables of Normalized Associated Legendre Polynomials," *Mathematical Tables Series*, Vol. 18, Pergamon Press, New York, N.Y., **1962**, 379 pp. (translation of *Tablitsy normirovannykh prisoyedinennykh polinomov Lezhondra*, U.S.S.R. Academy of Sciences, Moscow, 1956.)

Brenner, Norman, "Cooley-Tukey Fast Fourier Transform Codes," *File* No. System 360–20, Contributed Program No. 360D–13.4.001, Systems Reference library, IBM Corp., New York, N.Y., **1969**.

Eliasen, Erik, Machenhauer, Bennert, and Rasmussen, Erik, "On a Numerical Method for Integration of the Hydrodynamical Equations With a Spectral Representation of the Horizontal Fields," Department of Meterology, Copenhagen University, Denmark, **1970**, 35 pp. (unpublished report).

Ellsaesser, Hugh W., "Evaluation of Spectral Versus Grid Methods of Hemispheric Numerical Weather Prediction," *Journal of Applied Meteorology*, Vol. 5, No. 3, June **1966**, pp. 246–262.

Grimmer, M., and Shaw, D., "Energy-Preserving Integrations of the Primitive Equations on the Sphere," *Quarterly Journal of the Royal Meteorological Society*, Vol. 93, No. 397, London, England, July **1967**, pp. 337–349.

Kubota, S., Hirose, M., Kikuchi, Y., and Kurihara, Y., "Barotropic Forecasting With the Use of Surface Spherical Harmonic Representations," *Papers in Meteorology and Geophysics*, Vol. 12, No. 3/4, Meteorology Research Institute, Tokyo, Japan, Dec. **1961**, pp. 199–215.

Kurihara, Yoshio, "On the Use of Implicit and Iterative Methods for the Time Integration of the Wave Equation," *Monthly Weather Review*, Vol. 93, No. 1, Jan. **1965**, pp. 33–46.

Machenhauer, Bennert, Stanstead Seminar, McGill University, Montreal, Canada, July **1971** (private communication).

Merilees, Phillip E., "On the Linear Balance Equation in Terms of Spherical Harmonics," *Tellus*, Vol. 20, No. 1, Stockholm, Sweden, **1968***a*, pp. 200–202.

Merilees, Phillip E., "The Equations of Motion in Spectral Form," *Journal of the Atmospheric Sciences*, Vol. 25, No. 5, Sept. **1968***b*, pp. 736–743.

Orszag, Steven A., "Transform Method for Calculation of Vector-Coupled Sums: Application to the Spectral Form of the Vorticity Equation," *Journal of the Atmospheric Sciences*, Vol. 27, No. 6, Sept. **1970**, pp. 890–895.

Orszag, Steven A., "Numerical Simulation of Incompressible Flows Within Simple Boundaries: I. Galerkin Spectral Representations," *Studies in Applied Mathematics*, Vol. L, No. 4, M.I.T. Press, Cambridge, Mass., Dec. **1971**, pp. 293–327.

Phillips, Norman A., "Numerical Integrations of the Primitive Equations on the Hemisphere," *Monthly Weather Review*, Vol. 87, No. 9, Sept. **1959**, pp. 333–345.

Platzman, George W., "The Spectral Form of the Vorticity Equation," *Journal of Meteorology*, Vol. 17, No. 6, Dec. **1960**, pp. 635–644.

Robert, André J., "The Integration of a Low Order Spectral Form of the Primitive Meteorological Equations," *Journal of the Meteorological Society of Japan*, Ser. 2, Vol. 44, No. 5, Tokyo, Japan, Oct. **1966**, pp. 237–245.

Robert, André J., "Integration of a Spectral Barotropic Model From Global 500-Mb. Charts," *Monthly Weather Review*, Vol. 96, No. 2, Feb. **1968**, pp. 83–85.

Robert, André J., "Integration of a Spectral Model of the Atmosphere by the Implicit Method," *Proceedings of the WMO/IUGG Symposium on Numerical Weather Prediction, Tokyo, Japan, November 26-December 4, 1968*, Japan Meteorological Agency, Tokyo, Mar. **1969**, pp. VII–19—VII–24.

Silberman, Isadore, "Planetary Waves in the Atmosphere," *Journal of Meteorolgy*, Vol. 11, No. 1, Feb. **1954**, pp. 27–34.

[Received December 27, 1971; revised April 14, 1972]

UDC 551.326.1:551.507.362.2(261.43)"1972-321"

PICTURE OF THE MONTH
Spring Ice Migration Near Newfoundland

FRANCES C. PARMENTER—*Applications Group, National Environmental Satellite Service, NOAA, Suitland, Md.*

Satellite data has long been used for snow and ice surveillance. During spring 1972, satellites observed the formation, changes, and breaking-up of the pack ice along the Labrador Coast. According to the U.S. Naval Oceanographic Office (1972) and Kniskern (1972), the pack ice extended further south and east this year than at any other season during the last 20 yr. This year's increase in pack ice was attributed to the lower than normal (4–6°F below normal) temperatures during the winter and spring. A record accumulation of ice, 32 in. thick, was reported at St. Anthony, Newfoundland, in March.

This sequence of Automatic Picture Transmission (APT) photographs shows the changes in the ice along the north and east side of Newfoundland. On May 3 (fig. 1), an area of snow-covered ice (H–I–J) extended southeastward along the western shore of the Davis Strait to 47°W, east of Cape Bonavista. There appears to be no ice immediately along the coast in White or Notre Dame Bays (G). This ice became detached by the strong winds associated with a Low passage on the preceding day.

Another area of thin, grayer looking ice can be seen between Newfoundland and Anacosti Island (K–L). During the next 9 days, this ice decreased in size, leaving only a small area visible near shore on May 12 (K, fig. 2). Strong winds, associated with another Low that passed directly over Newfoundland, have changed the configuration of the south end or string of ice in figure 2. Northerly winds pushed ice westward into White Bay (G) and strong southerly winds east of the island moved the ice northward between I and J (fig. 2).

More moderate weather dominated the region during the following 2 weeks. Southerly flow predominated, and a warming trend with temperatures in the 50s was reported. In the APT photograph taken on May 25 (fig. 3), the string of ice (I–J) had moved south and east of its earlier position as a result of advection by the southward flowing Labrador Current. Ice still remained along the shore in White and Notre Dame Bays.

On May 26 another intense Low passed over Newfoundland, bringing strong northerly winds over the area. The string of ice (I–J) seen in figure 4 continued to move southward, but some thinner spots began to appear near L.

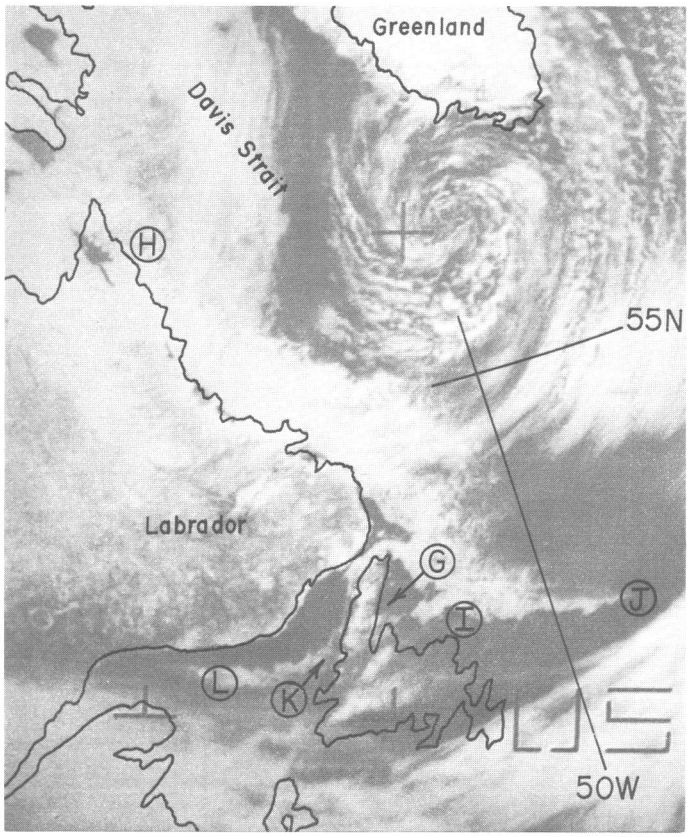

FIGURE 1.—ESSA 8 photograph, orbit 15503 on May 3, 1972, at 1433 GMT.

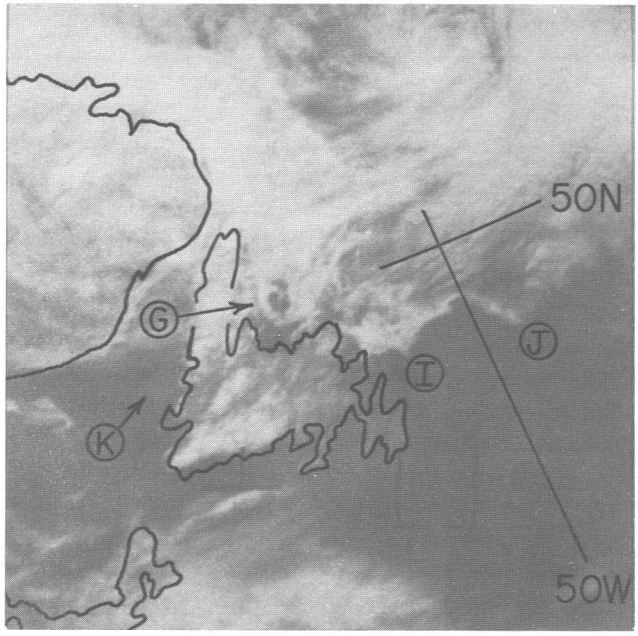

FIGURE 2.—ESSA 8 photograph, orbit 15616 on May 12, 1972, at 1435 GMT.

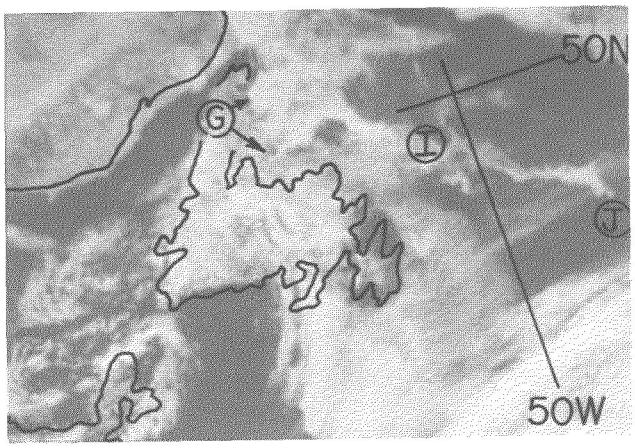

FIGURE 3.—ESSA 8 photograph, orbit 15779 on May 25, 1972, at 1417 GMT.

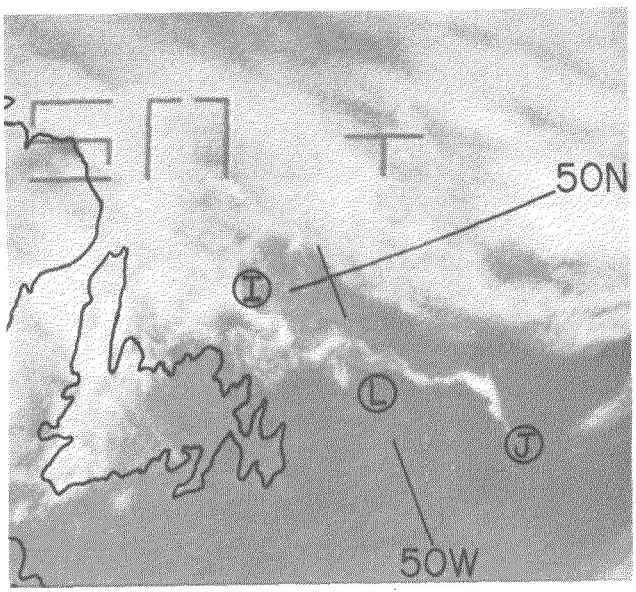

FIGURE 4.—ESSA 8 photograph, orbit 15804 on May 27, 1972, at 1405 GMT.

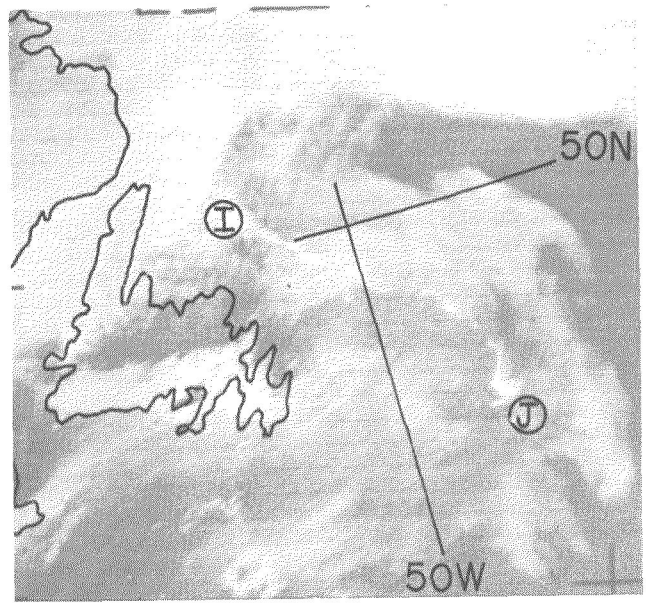

FIGURE 5.—ESSA 8 photograph, orbit 15854 on May 31, 1972, at 1340 GMT.

The farthest southern extent of the ice was seen on May 31. The string of snow-covered ice (I–J, fig. 5) can be seen through a thin overcast of low clouds. Heavier cloud cover prevented further satellite observation of the ice after that date.

Satellites continue to provide ice information to users throughout the world. In addition to the Arctic example shown here, satellite data is being used in the Pacific for Alaskan shipping and in the Antarctic for resupply missions.

REFERENCES

Kniskern, Frank, U.S. Naval Oceanographic Office, Washington, D.C., June 22, 1972 (personal communication).

U.S. Naval Oceanographic Office, *Eastern Arctic Ice Seasonal Outlook 1972*, SP-60(72), Washington, D.C., Apr. 1972, 12 pp.